



ULTIMATE BEHAVIOR OF SEISMICALLY ISOLATED NPP

Nadim Moussallam¹, Bastien Boudy², Andreas Schellenberg³

¹ Expert Engineer in Seismic and Dynamic Analysis, AREVA NP, Germany

² Engineer in Seismic and Dynamic Analysis, AREVA NP, France

³ Research Engineer, University of California at Berkeley, USA

ABSTRACT

Because of increased seismic demand on Nuclear Power Plants (NPP) due to both regulatory changes and new projects in high seismicity countries, a significant interest in Seismic Isolation Systems (SIS) has developed in recent years. Still, and except in France, very few projects of completely isolated NPP have actually been implemented. This is partly due to the apparent lack of internationally recognized codes and standards for application of SIS to the nuclear industry. The present paper has the objective of drafting a possible justification approach for application of SIS to NPP, with a particular focus on predicting its ultimate seismic behaviour and including it in the overall safety demonstration of the plant.

INTRODUCTION

Seismic isolation technologies are used for the seismic protection of nuclear structures since the late 70s in France. Isolated plants include the 4 Cruas 900 MW pressurized water reactors, the experimental Jules Horowitz and ITER reactors, the La Hague fuel storage pools and the GBII uranium enrichment facility. A detailed overview of this experience can be found in AFCEN (2014). In all these cases, simple polychloroprene laminated rubber bearings were used as isolators. A significant advantage of this technology is that its behaviour, in most cases and for moderate seismicity, can safely be approximated as being linear. The seismic safety demonstration, for these plants, was then carried out with applying the same methodologies as for a usual NPP design.

For countries with significantly higher seismic demand, the use of simple laminated rubber bearings is difficult, due to the potentially large seismically induced isolator deformations. In these cases, addition of energy dissipation devices is necessary. One of the simplest ways to dissipate energy is the addition of lead plugs directly inside the laminated rubber bearings. The so called Lead plug Rubber Bearing (LRB) constitutes one of the most commonly envisaged technologies for new isolated NPP on sites with high seismic demand.

However, the dynamic behaviour of a NPP isolated with LRB can be highly nonlinear and the standard justification methodologies that were applied for existing isolated plants cannot readily be re-conducted. Besides, there are no internationally recognized codes and standards for application of such systems to NPP. The present paper gives one possible justification approach for the application of LRB based SIS to NPP, including the construction of an adequate numerical model, its experimental validation based on comparison with characterization and hybrid test results, and, finally, the estimation of the ultimate seismic behaviour of the isolated NPP.

The paper is based on an example case that was provided by KEPCO E&C as part of an IAEA international benchmark on hybrid simulation of SIS for application to NPP, described by Lee (2016). This example case included a given type of LRB, a building model representing a complete NPP and several spectral-matched ground motions corresponding either to the US NRC RG-1.60 (2014) spectral shape or to the EUR (2012) spectral shape for hard soil conditions. Experiments were conducted by the Pacific Earthquake Engineering Research (PEER) Center at the UC San Diego Seismic Response Modification Device (SRMD) laboratory (2014).

NUMERICAL MODEL FOR LEAD RUBBER BEARING ISOLATORS

Global approach

The development of an adequate numerical model of a single isolator is the first necessary step in the global isolated NPP seismic safety demonstration. Such isolator model is to be inserted in the global NPP finite element analysis model between the upper basemat, constituting the foundation of the isolated superstructure, and the lower basemat, supporting the isolation system. In practice, during an earthquake excitation, each isolator will be subjected to a different set of loads resulting from:

- The differential distribution of vertical loads originating from the superstructure vertical seismic response and due to the necessarily non-perfect fit between the isolator positions and the superstructure weight distribution.
- The rocking motions induced by the superstructure rotary inertia and the height of the superstructure centre of mass with respect to the seismic isolation level.
- Possibly the torsional motions of the superstructure, when a horizontal in-plane offset exists between its centre of mass and the centre of stiffness of the seismic isolation system.

It is therefore necessary to model each isolator individually. Besides adequately reproducing the main isolator characteristics, the individual isolator numerical model should also remain simple enough so that a large number of them (typically several hundreds) could be implemented into the global NPP model with keeping this model industrially viable.

Numerous research programs have been conducted worldwide on the behaviour of LRB, notably by the MCEER institute at the University of Buffalo (see Constantinou 2007) and the PEER institute at the University of Berkeley (see Schellenberg 2015). From these research programs, the main features of the seismic behaviour of LRB isolators are now well known. They include:

- The **shear behaviour** of the isolator, including its dependency on vertical loads and cyclic shear distortion (heating of the lead core with successive incursions into the plastic domain)
- The **tensile behaviour** of the isolator, including the onset of cavitation in the rubber volume (formation of micro-cracks permanently affecting the vertical tensile stiffness)
- The **compressive behaviour** of the isolator and its dependency on horizontal isolator distortion (reducing both the vertical stiffness and the critical buckling load)

The numerical model developed should be able to represent all these characteristics, but in a simplified manner.

Additionally, the possible rubber characteristic's variation with time (ageing), with temperature, or the variations due to uncertainties in the manufacturing process should be quantified and these variations should be acknowledged in the design process. To do so, it is suggested to define at least two bounding cases corresponding to the minimal and maximal expected rubber stiffness during the lifetime of the isolation system considering extreme temperature variations at the plant site. The complete analysis is then to be performed in parallel with a reference "mean" case and with these two bounding cases.

Example of application

An example LRB isolator with multiple lead cores (see Figure 1) was considered in developing the numerical model presented herein. This example was provided by KEPCO E&C as part of an IAEA international benchmark on hybrid simulation of SIS for application to NPP and is described in Lee (2016). The dimensions of the example LRB are given in Table 1. A numerical model of this isolator was implemented in Matlab and subsequently used for the seismic analysis of a complete NPP isolated with 486 bearings.

Table 1: Example LRB dimensions (Courtesy of KEPCO E&C)

External diameter (mm)	1520
Diameter of equivalent lead core (mm)	400
Thickness of rubber layers (mm)	7
Thickness of steel reinforcing layers (mm)	7
Number of rubber layers	30
Total height of bearing (mm)	533

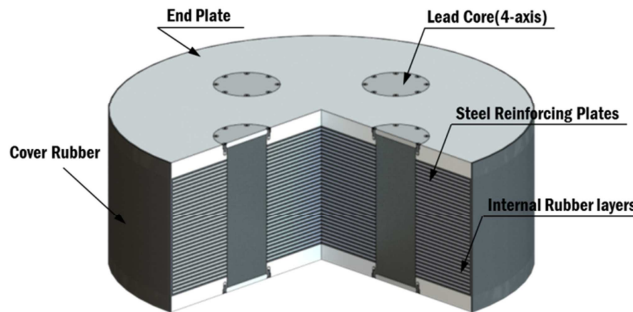


Figure 1. Example LRB (Courtesy of KEPCO E&C)

Model for shear behaviour

The isolator pure shear behaviour is represented using a Bouc-Wen model as developed by Park et al (1986) for hysteretic systems under bi-directional ground motions. The calculation of the restoring forces F_x and F_y is performed as detailed in equations 1 and 2 below. The resulting hysteresis behaviour is illustrated in Figure 2a.

$$\begin{pmatrix} F_x \\ F_y \end{pmatrix} = C_d \cdot \begin{pmatrix} \dot{U}_x \\ \dot{U}_y \end{pmatrix} + K_d \cdot \begin{pmatrix} U_x \\ U_y \end{pmatrix} + (\sigma_{YL} * A_L) \cdot \begin{pmatrix} Z_x \\ Z_y \end{pmatrix} \quad (1)$$

$$Y \cdot \begin{pmatrix} Z_x \\ Z_y \end{pmatrix} = \left([I] - \begin{pmatrix} Z_x^2 (\gamma \text{Sign}(\dot{U}_x Z_x) + \beta) & Z_x Z_y (\gamma \text{Sign}(\dot{U}_y Z_y) + \beta) \\ Z_x Z_y (\gamma \text{Sign}(\dot{U}_x Z_x) + \beta) & Z_y^2 (\gamma \text{Sign}(\dot{U}_y Z_y) + \beta) \end{pmatrix} \right) \cdot \begin{pmatrix} \dot{U}_x \\ \dot{U}_y \end{pmatrix} \quad (2)$$

Where K_d is the linear shear stiffness of the isolator, C_d is the linear equivalent viscous damping representing the energy dissipation in the rubber (here set to achieve a 2% ratio of critical damping, typical of natural rubber), U and \dot{U} are the relative displacement and velocity between the upper and lower end plate of the isolator, σ_{YL} and A_L are the lead core's effective yield stress and cross sectional area respectively, and Y is the yield displacement. The γ and β parameters control the hysteresis loop shape and can be calibrated based on experimental characterisation tests. $\gamma = 0.1$ and $\beta = 0.9$ were adopted in the present case.

The alternating nature of the seismic excitation gives rise to cyclic loads within the lead cores. With each cycle, energy is dissipated in the form of heat. During a seismic event, the rubber acts as a coating material to the lead and the heat that accumulates in the lead can only be dissipated through the isolator's steel shim plates. However, most of it remains trapped in the lead itself, leading to a progressive decrease of its effective yield stress, σ_{YL} . This effect is included within the model based on the equations developed by Kalpakidis et al (2010):

$$\sigma_{YL}(T_L) = \sigma_{YL0} e^{-E_2 T_L} \quad (3)$$

Where σ_{YL0} is the yield stress at the reference temperature, E_2 is an experimental parameter predicting the instantaneous yield stress as a function of the temperature, and T_L is the temperature of the lead core, with value increasing with increasing accumulated plastic deformation of the lead. Input data to the model include the lead core dimensions, the specific heat and density of lead, the thermal diffusivity, thermal conductivity and total thickness of the steel shim plates. The effect of the lead plug heating is illustrated in Figure 2b.

The isolator shear stiffness K_d may be affected by the vertical compressive load. This phenomenon is captured by making the shear stiffness a function of the vertical load, as proposed by Kumar et al (2014). The model used is given in equation 4 and illustrated in Figure 2d.

$$K_d = K_{d0} * \left[1 - \left(\frac{P}{P_{cr}} \right)^2 \right] \quad (4)$$

Where P is the compressive load on the isolator, P_{cr} is the critical buckling load and K_{d0} is the theoretical shear stiffness with no influence on the vertical load. The buckling load P_{cr} is itself determined as a function of the isolator distortion according to the model developed by Buckle and Liu (1993). Variation of the buckling load with horizontal distortion is illustrated in Figure 2c.

Finally, the possible hardening of the rubber under extreme shear distortion has not been modelled in the present example. Such effect could be implemented by adding a dependency of the K_d parameter to the shear distortion above a certain experimentally determined threshold.

Model for tensile behaviour

The isolator vertical behaviour under tensile load is a linear force-displacement response up to reaching the rubber cavitation limit. The first loading beyond the cavitation limit causes a decrease of the vertical stiffness due to the creation of new micro-cracks in the rubber. The axial unloading path is then different from the previous one and a new cavitation limit is set at the point that was reached during this cycle. Each subsequent cycle exceeding the new cavitation point creates a new force-displacement response with a new unloading path. The post-cavitation force F is calculated as developed in Kumar et al (2014) and reproduced in equation 5 below. The resulting tension behaviour is illustrated, for several successive cycles, in Figure 2e.

$$F(u) = F_C \left[1 + \frac{1}{kT_r} \left(1 - e^{-k(u - \frac{F_C}{K_v})} \right) \right] \quad (5)$$

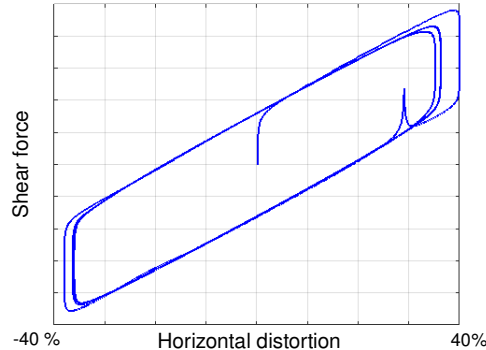
Where F_C is the cavitation force, K_v is the linear tensile stiffness, T_r is the total rubber thickness, u is the post cavitation displacement and k is a parameter defining the shape of the post-cavitation variation of the tensile stiffness. A damage index is defined to consider the effect of cycling cavitation.

Model for compressive behaviour

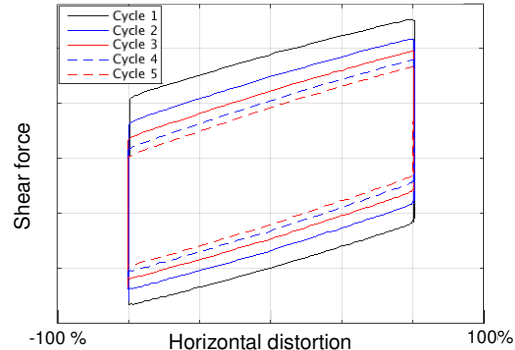
The isolator vertical behaviour under compressive load is affected by the horizontal distortion of the isolator, because the effective area of the isolator in compression is reduced by such distortion. The variation of the axial compressive stiffness is modelled by equation 6, extracted from the work of Warn et al (2007). The behaviour is illustrated in Figure 2f.

$$K_v = K_{v0} * \left[1 + \frac{3}{\pi^2} * \left(\frac{u_h}{r} \right)^2 \right]^{-1} \quad (6)$$

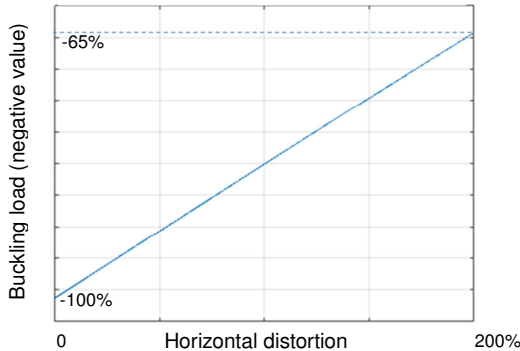
Where K_{v0} is the vertical stiffness at zero horizontal distortion, u_h is the horizontal displacement and r is the radius of gyration of the bonded rubber area.



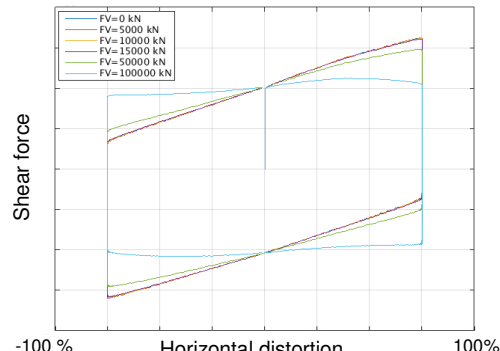
a) Pure horizontal shear behaviour of the model,
 without temperature effect



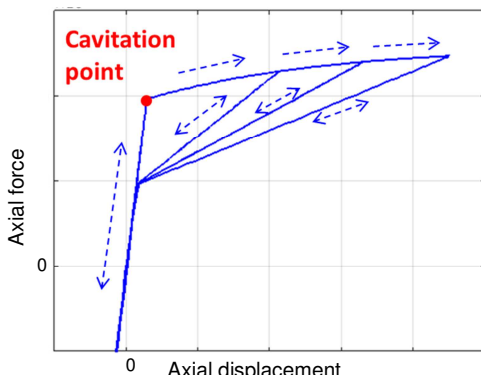
b) Pure horizontal shear behaviour of the model,
 with temperature effect



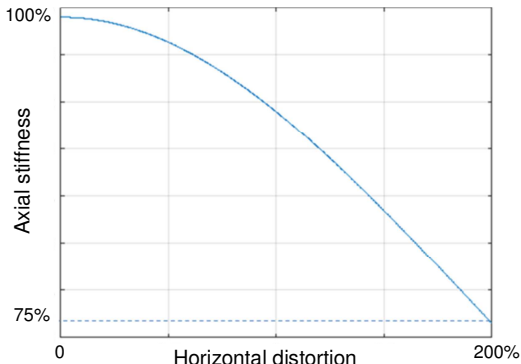
c) Variation of axial buckling load as a function of
 horizontal distortion



d) Effect of vertical load on the horizontal shear
 behaviour



e) Isolator cavitation behaviour under tensile load



f) Variation of axial compressive stiffness as a
 function of horizontal distortion

Figure 2. Overview of the behaviour of the numerical isolator model

CALIBRATION AND VALIDATION OF NUMERICAL MODEL

After defining the numerical model for the LRB, as presented in the previous chapter, it is necessary to calibrate this model and to validate it. A possible approach to do so is to:

- Perform elementary characterisation tests on a full scale bearing to calibrate the model.
- Perform response history loading tests on a full scale bearing, with loads representative of seismic loading conditions, in order to validate the previously calibrated model.

Each of these steps is described in one of the following paragraphs.

Calibration through characterisation tests

Although most of the dynamic characteristics of an LRB isolator can be deduced from the knowledge of its dimensions and material properties, a calibration of certain parameters, based on experimental characterisation tests is recommended. This is notably the case for the Bouc-Wen γ and β hysteresis loop parameters, the tensile behaviour k parameter, the cavitation force F_C and the representation of hardening, when such behaviour is included in the model. The calibration is generally performed by graphical fitting of the numerical hysteresis curves on the experimentally obtained ones. An example of the calibration process, performed by PEER based on the characterisation tests of the example LRB, is illustrated in Figure 3. The LRB-BW numerical model represents an isolator that does not include temperature effects and the LRB-X numerical model corresponds to the modelling approach described in detail above.

Besides, it is highly recommended to derive the vertical reference stiffness value K_{v0} from the experimental characterisation tests instead of using theoretical formulae such as those given in generic codes and standards for elastomeric bearings. It has indeed been observed that analytical formulae, although fully acceptable for determining the isolators' horizontal stiffness, were often not capable of accurately predicting their vertical stiffness. Finally, it is recommended to at least verify the correct functioning of the Kalpakidis et al (2010) model for lead heating with cyclic loading when applied to particular isolators, such as the one with four lead cores considered in this study.

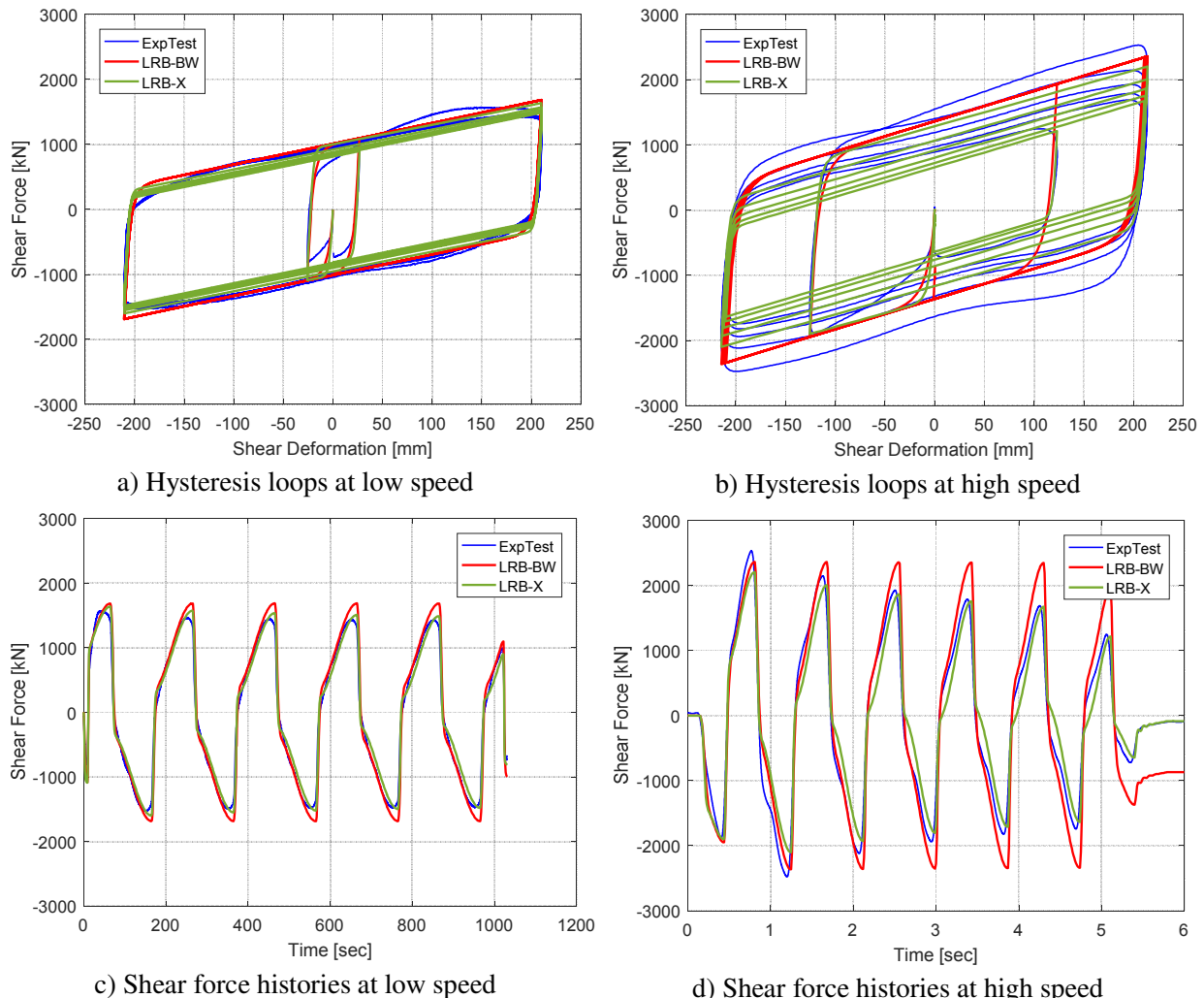
Validation based on hybrid test results

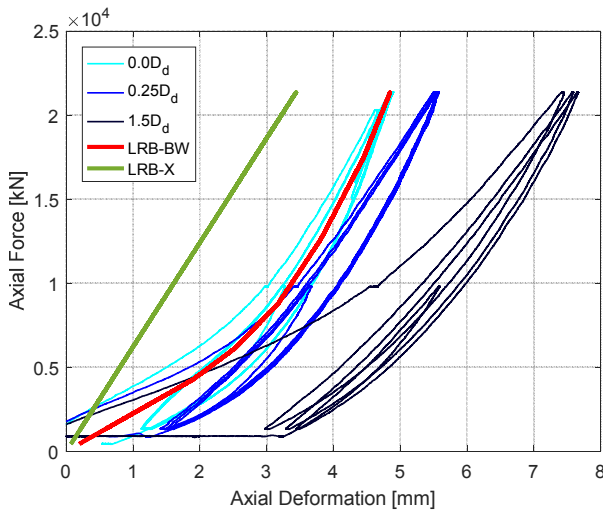
The validation of a LRB model for the seismic isolation of a NPP can obviously not be performed using a full-scale model of the isolated plant. It is also not possible to conduct it using reduced-scale models of the plant and of the isolation system since the scaling factors cannot be established for all parameters at the same time: horizontal stiffness, vertical stiffness, lead yield, tensile behaviour, buckling loads...

Hybrid simulation tests offer a possible workaround to these shortcomings. In a hybrid test, one single full-scale isolator is tested and the response of the rest of the system (super-structure, infrastructure and, possibly, other isolators) is simulated in real time. This experimental testing technique allows the application of best estimated time history loads on the tested isolator while recording its response and feeding such response back into the numerical model. Two types of complementary approaches can be adopted: either the tested isolator alone represents all of the isolation system, or the tested isolator represents only one isolator of the system, while the others are being simulated. In the first case, there is no influence of the isolator numerical model on the loads applied to the tested isolator, but this approach is unable to represent rocking and torsional motions of the superstructure that would result in differential loading of the different isolators. In the second case rotational motions are represented but there is practically no more influence of the tested isolator, which is only one among many, on the overall simulated structural response. Still, if the hysteresis curves obtained for the simulated and tested isolators are comparable, and if the in-structure response spectra obtained with the full simulation and with the hybrid test simulation are comparable, the basis for validating the numerical model is established.

Figure 4 illustrates the comparison between the results of the purely numerical model set up by AREVA NP, as defined in the previous chapter, and hybrid tests performed by PEER as part of the IAEA benchmark. The comparison is made for floor response spectra obtained at the uppermost point of one of the superstructure models (Node 6715) when applying a 0.5 g PGA seismic excitation with US NRC RG-1.60 (2014) spectral shape. Due to physical limitations of the test rig, two tests were conducted by PEER: Test 1 was performed in real time, but with no vertical excitation and Test 2 was performed at an extended time scale allowing to apply the vertical excitation simultaneously with the horizontal ones. In these tests, one isolator was set to represent the complete isolation system and horizontal excitations were applied in both X and Y directions.

For the example of application presented here, no calibration of the AREVA NP isolator model was performed preliminary to the hybrid testing. This is because the calculations were part of an IAEA organized blind benchmark. The results are nonetheless quite comparable to the ones obtained by PEER, and, indeed, within the variation range of the available experimental results themselves (comparison between Test 1 and Test 2). From a designer's point of view, such comparison could already be used as a basis for validation, even though it should be complemented with experimental test results obtained with other, and especially higher seismic excitations.





e) Variation of axial compressive stiffness as function of horizontal distortion

Figure 3. Calibration process of the LRB-BW and LRB-X numerical models

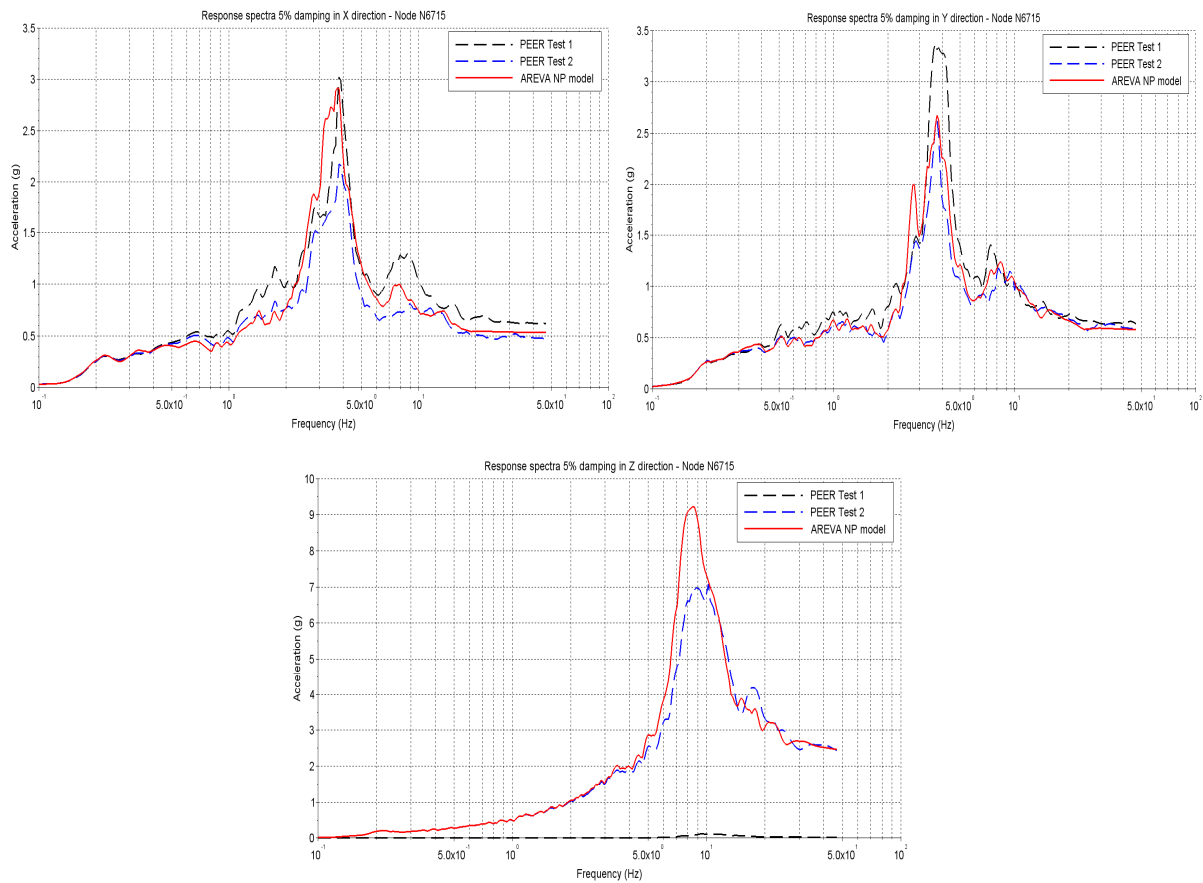


Figure 4. Validation of the numerical model – Comparison with results from hybrid tests

DETERMINATION OF ULTIMATE BEHAVIOR AND SAFETY DEMONSTRATION

Overall proposed approach

The first step in the design and justification of a SIS for a NPP is the verification that the applicable code's and standard's criteria are respected for a design basis seismic event. In the European context, and for an isolation system with LRB isolators, these criteria can be found in the EN 15129 (2010) and the EN 1337-3 (2007) European standards. Historically, safety authorities have required that more stringent criteria be applied to elastomeric bearing designs for the isolation of NPP, as described in AFCEN (2014). Doing so, larger margins are ensured for nuclear structures compared to non-nuclear ones for a design basis event.

In present times, respecting the code's and standard's design criteria for a design basis event is not sufficient anymore. Indeed, it is required that the beyond design margins are explicitly assessed, that the ultimate capacity of the isolation system is known, and, in some cases, that the fragility of the system (probability of failure as a function of the excitation amplitude) is estimated. A possible way to perform such demonstrations consists in:

- a) Determining the ultimate behaviour of a single isolator based on a limited number of destructive tests. The limits to be assessed are the ultimate shear failure limit, the ultimate tensile failure limit, the ultimate buckling failure limit and the failure limits under combined tension-shear and compression-shear. Obviously not all combinations can be tested and the choices of the destructive tests to be performed need to be made based on the expected behaviour of the isolated NPP. As an example, it may not be required to precisely assess the buckling loads if the numerical simulations show that other limits will be reached first.
- b) Drawing the failure limit of the isolator on a graph of shear deformation versus axial loads. The experimental points determined earlier are put on this graphs and interpolation is performed between these points to draw the lines defining the capacity limit of the isolator. Several sets of parallel lines could be drawn to represent the uncertainty on the ultimate limits due to ageing, temperature, environmental conditions and manufacturing variability.
- c) Running multiple response-history calculations with continuous increase of the excitation level (incremental dynamic analyses). For each isolator, each time history can be represented in the shear deformation versus axial load graph defined earlier. The isolator is considered to be lost as soon as the time history curve crosses over one of the failure limit lines. The calculation can either be stopped or be continued until enough isolators are lost to constitute a global failure of the entire isolation system.

As a result, a multiplicative factor on the Design Basis Earthquake (DBE) can, alone, express the beyond design capacity of the complete isolation system. An identical approach could be adopted for a probabilistic analysis, performing multiple analyses for each multiplicative factor of DBE loads with randomization of the leading parameters.

Example application case

Figure 5 illustrates a partial application of the overall methodology to the particular case of the IAEA international benchmark described in Lee (2016). The left side of this figure corresponds to a progressive scaling of a time history loading matched to the US NRC RG-1.60 spectrum. The right side of this figure corresponds to a progressive scaling of a time history loading matched to the EUR spectrum for hard soil conditions. In this case, the failure limits constituted by red lines were set up based on literature results instead of actual destructive testing. For the US NRC RG-1.60 spectral shape, the failure occurs in shear for loading equal to or higher than 2 DBE. For the EUR hard spectral shape, the failure occurs due to a combination of shear and tension for loading equal to or higher than 4 DBE. These graphs illustrate the different behaviours that are observed for a same isolated structure subjected to different

seismic inputs. They can serve as a tool to optimize the SIS design for one site with one given response spectrum shape.

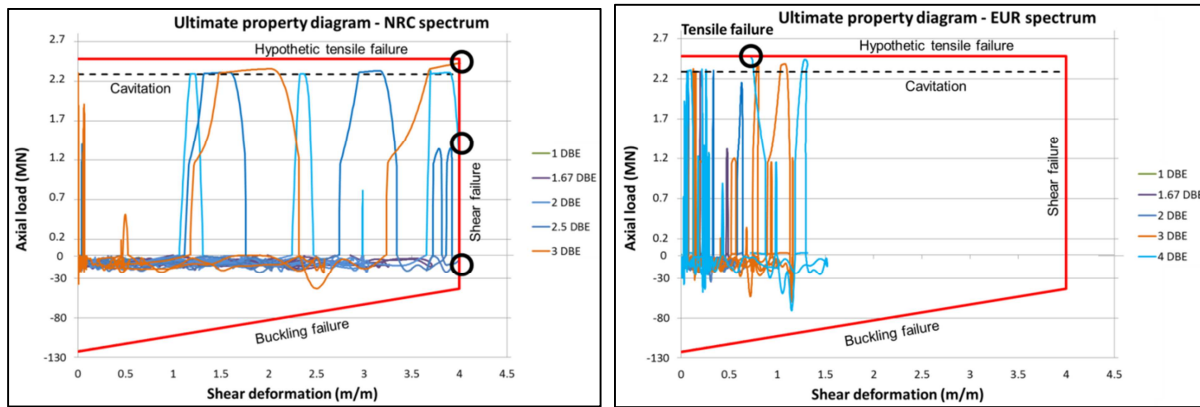


Figure 5. Graphical view of the determination of ultimate behaviour

CONCLUSION

The present paper provides a possible holistic approach to demonstrate the safety of a seismically isolated NPP. This demonstration includes the construction of a numerical model able to represent the key behaviour of each isolator, a calibration of this model based on characterisation tests, a validation of this model based on comparison between numerical analyses and hybrid test results, an experimental determination of the individual isolator ultimate capacity, and, finally, an assessment of the ultimate capacity of the isolated NPP based on graphical comparison between the results of multiple response history numerical analyses and experimentally obtained ultimate capacity limits.

Part of this approach was set in place by AREVA NP for the example of the IAEA benchmark described in Lee (2016). A Matlab model for a LRB isolator was developed and integrated hundreds of times into a complete NPP model. Even though the model was not calibrated in this case, comparison with results of hybrid tests conducted by PEER showed relatively good agreement. Multiple response history analyses, with incrementally increasing loading conditions, were then performed to determine the ultimate capacity of the isolated NPP. This example demonstrates the industrial feasibility of the proposed approach.

REFERENCES

- AFCEN PTAN RCC-CW Technical Publication “French Experience and Practice of Seismically Isolated Nuclear Facilities.” Edition 2014
- Buckle, I.G., Liu, H., (1993), “Stability of elastomeric seismic isolation system”, *Proceedings of the seminar on Seismic Isolation, Passive Energy Dissipation, and Control*, 293-305.
- Constantinou M. C., Whittaker, A.S., Kalpakidis, Y., Fenz D.M., Warn G.P. (2007), *Performance of Seismic Isolation Hardware under Service and Seismic Loading*, MCEER report ISSN 1520-295X
- European Utility Requirements for LWR Nuclear Power Plants (EUR) (2012), “Generic Nuclear Island Requirements”, Chapter 4, Design Basis.
- European standard EN 1337-3 (2005) Structural bearings
- European standard EN 15129 (2010) Anti-seismic devices
- Kalpakidis, I. V., Constantinou, M. C., and Whittaker, A. S. (2010). “Modeling strength degradation in lead-rubber bearings under earthquake shaking”, *Earthquake Engineering & Structural Dynamics*, 39:1533-1549.

- Kumar, M., Whittaker, A., and Constantinou, M. C. (2014). "An advanced numerical model of elastomeric seismic isolation bearings", *Earthquake Engineering & Structural Dynamics*, 43:1955-1974.
- Kumar, M., et al., (2015). "Response of base-isolated nuclear structures to extreme earthquake shaking." *Nucl. Eng. Des.* 295:860-874.
- Lee, S. H., (2016) "Hybrid Simulation to Assess Performance of Seismic Isolation in Nuclear Power Plants – International Benchmark Program", *Proceedings of the TINCE-2016 conference, Paris*
- Park, Y.J., Wen, Y.K., Ang, A.H.S, (1986) "Random vibration of hysteretic systems under bi-directional ground motions." *Earthquake Eng. Struct. Dyn.* 14 (4), 543-557.
- Schellenberg, A. H., Sarebanha, A., Schoettler, M. J., Modqueda, G., Benzoni, G., and Mahin, S. A. (2015). "Hybrid Simulation of Seismic Isolation Systems Applied to an APR-1400 Nuclear Power Plant". Technical Report PEER 2015/05 Pacific Earthquake Engineering Research Center, University of California, Berkeley, Berkeley, CA
- UCSD. (2014). Caltrans seismic response modification device (SRMD) test facility. University of California, San Diego. <Available from <http://structures.ucsd.edu/node/62>>
- USNRC, (2014) "Design response spectra for seismic design of nuclear power plants", Regulatory Guide 1.60, Revision 2.
- Warn, G., Whittaker, A. S. and Constantinou, M. C. (2007), "Vertical Stiffness of Elastomeric and Lead-Rubber Seismic Isolation Bearings", *Journal of Structural Engineering*, 133(9):1227-1236.